Characterization of Recombinant Human Erythropoietin Produced in Chinese Hamster Ovary Cells†

Janice M. Davis and Tsutomu Arakawa*
Protein Biophysics, Amgen, Thousand Oaks, California 91320
Thomas W. Strickland
Protein Biochemistry, Amgen, Thousand Oaks, California 91320
David A. Yphantis*
Department of Molecular and Cell Biology, University of Connecticut, Storrs, Connecticut 06268, and Department of Biology and Institute of Molecular Biology and Biotechnology, University of Crete, Iraklion, Crete
Received November 17, 1986

ABSTRACT: Physicochemical properties of recombinant human erythropoietin were examined. This protein, produced in Chinese hamster ovary cells, showed a conformation apparently identical with the natural product isolated from human urine when examined by circular dichroism, UV absorbance, and fluorescence spectroscopy. Sedimentation equilibrium experiments showed the recombinant erythropoietin preparation to be essentially a single macromolecular component with a molecular weight of 30 400 and a carbohydrate content of 39%. The Stokes radius of recombinant erythropoietin was estimated to be 32 Å from gel filtration, much larger than the 20-Å radius calculated for a sphere of the observed molecular weight. This difference may be ascribed to the extensive glycosylation. The fluorescence and phosphorescence spectra showed that the luminescent tryptophan(s) is (are) solvent-exposed and can be quenched by I^- and acrylamide but not by Cs^+. On acid titration, the recombinant erythropoietin showed a conformational transition with a midpoint of pH 4.1. This suggests that the net charges on the protein moiety rather than on the whole molecule play a role in protein structure stability.

Erythropoietin (EPO),[1] a glycoprotein produced primarily by the kidney, is the principal regulator of red blood cell formation. Human EPO has been purified from the urine of patients with aplastic anemia (Miyake et al., 1977). Although the biological effects are relatively well-known, little is known about the biochemical and biophysical properties of EPO, largely because insufficient quantities of the protein are obtainable from the natural sources. Recently, the amino acid sequence of human EPO was determined (Lai et al., 1986) and a gene coding for human EPO cloned (Lin et al., 1985; Jacobs et al., 1985). The corresponding protein was expressed in Chinese hamster ovary cells and purified by sequential chromatography. This provided an ample quantity of highly purified protein for extensive structural characterization. Recombinant EPO, like the natural material isolated from urine, is a glycoprotein and exhibits biological activity in both in vivo and in vitro assays (Lin et al., 1985). We have characterized the structure of recombinant EPO by a number of physicochemical techniques including circular dichroism, luminescence spectroscopy, gel filtration, and sedimentation equilibrium, comparing the results with those for the natural protein where possible.

Materials and Methods

Recombinant human EPO was purified from CHO cell conditioned media by a series of chromatographic procedures to greater than 95% purity. The following experiments were carried out in 20 mM sodium citrate buffer, pH 7, and 0.1 M NaCl, except as otherwise indicated. Protein concentration was spectrophotometrically determined by using an extinction coefficient of 0.743 for the whole EPO molecule (at 280 nm at 0.1% solution). This extinction coefficient (for the whole molecule) was determined by a dry weight procedure (Kupke & Dorrier, 1978).

Circular dichroism was determined with a Jasco J-500C spectropolarimeter at room temperature. The data were expressed as mean residue ellipticity calculated by using a mean residue weight of 111 for the protein moiety. The UV absorbance spectrum was determined on a Hewlett-Packard Model 8451A diode array spectrophotometer. This device subtracts the base line and generates derivatives of absorbance with regard to wavelength at 2-nm intervals. Luminescence spectra were determined on a Perkin-Elmer LS-5 fluorescence spectrophotometer. Fluorescence spectra were determined at room temperature. Phosphorescence spectra were determined at liquid nitrogen temperature (nominally 77 K) using fused silica tubes with an inner diameter of 2 mm. The samples were mixed with 1 volume of ethylene glycol.

Fluorescence quenching experiments were performed by using acrylamide of electrophoresis purity from Bio-Rad, KI from Sigma, and CsCl of optical grade from Gallard–Schlesinger. The cell was maintained at 21 °C. A 0.5-cm cuvette was used. Small volumes of a concentrated stock solution of acrylamide were added to an EPO solution. Excitation was at 300 nm to minimize acrylamide absorbance. The absorbance of the EPO solution in the acrylamide quenching experiments was 0.15 at 300 nm. Separate samples were prepared for each quencher concentration for KI and CsCl

† A preliminary report of part of this work has been presented at the 30th Annual Meeting of the Biophysical Society, San Francisco, CA, Feb 12, 1986.

[1] Abbreviations: EPO, erythropoietin; CD, circular dichroism; rpm, revolutions per minute; SDS, sodium dodecyl sulfate; CHO, Chinese hamster ovary; FWHM, full width at half-maximum.

0006-2960/87/0426-2633$01.50/0

quenching experiments: appropriate volumes of 4 M NaCl and a 4 M solution of the ionic quencher were added so that the ionic strength of each sample was the same. Excitation was at 300 nm (where the absorbance of the EPO solution was about 0.08) for the KI quenching experiments and at 280 nm (with an EPO absorbance of about 0.1) for CsCl quenching. Corrections were made for dilution and for absorbance by the quencher: $F^{cor} = F^{obsd}10^{\Delta A/2}$, where ΔA is the change in the absorbance by addition of the quencher (Lehrer & Leavis, 1978).

Acid denaturation of recombinant EPO was examined by dialyzing the protein solution against 25 mM citrate and 0.1 M NaCl of the appropriate pH.

Gel filtration was carried out on a Sephacryl S-200 column (3.2 cm × 51 cm) equilibrated with 20 mM sodium citrate, pH 7, and 0.1 M NaCl. The column was calibrated with four proteins of known Stokes radii: cytochrome *c* (16.4 Å), ribonuclease (19.2 Å), ovalbumin (27.3 Å), and human serum albumin (34.9 Å). These Stokes radii were taken from Laurent and Killander (1964). The elution parameter, $K_{av} = (V_e - V_0)/(V_t - V_0)$, was analyzed according to the partition theory developed by Ogston (1958), where V_e, V_0, and V_t are the elution, void, and total volumes in the column, respectively.

Sedimentation equilibrium experiments were performed on a Model E ultracentrifuge (Beckman Instruments Co.) equipped with a pulsed argon ion laser (Paul & Yphantis, 1972), a digital laser controller (Yphantis et al., 1984), and an automated control system for photography (Laue et al., 1984). External loading cells (Ansevin et al., 1970) with three pairs of channels and a 30-mm optical path length were used at speeds of 22000, 30000, and 40000 rpm. Blanks were run before and after the runs at all speeds to correct for optical distortions. Loading concentrations were 0.09, 0.23, and 0.62 g/L, and solution column heights were about 2.6 mm. The centrifugation times exceeded (by factors of 1.1–8) estimates of the time required to attain equilibrium obtained according to van Holde and Baldwin (1958) with $\epsilon = 0.001$ assuming a (worst case) diffusion coefficient of 6×10^{-7} cm^2 s^{-1}.

Rayleigh interferograms were taken on "Technical Pan" 35-mm film (Kodak 2415) and were measured with a PDP-8/L minicomputer controlled system [see Laue and Yphantis (1979), T. M. Laue and D. A. Yphantis (unpublished results), and Laue (1981)] that provides estimates of fringe displacement as a function of position. Typically, the images were measured every 8 μm on the images (corresponding to about 4-μm intervals in the ultracentrifuge). Data analyses were performed by using nonlinear least-squares approaches (Johnson et al., 1981) with various assumed models. The indicated ranges of the fitting parameters in each case correspond to a confidence range of about 65% probability. (For Gaussian error distributions, these 65% confidence regions are equivalent to ranges of the mean plus or minus one standard deviation.) The programs used were derived from a version of the NONLIN programming system written in Fortran for a Digital Equipment Co. (DEC) PDP 11/23 system (M. L. Johnson, private communication). Some of these programs were also adapted for use under VMS on a DEC VAX 11/780 system. Apparent z-average molecular weights for each channel at each speed were estimated from nonlinear least-squares fits of the fringe displacements in a solution channel to a model of a single ideal component. This procedure is similar to an orthogonal linear least-squares procedure (Correia, 1980, 1983; J. J. Correia and D. A. Yphantis, unpublished results) and can be shown to be equivalent to an estimation of $M_{z,app}$ from the ratio of the second derivative to the first derivative of the fringe displacement (Yphantis, 1964).

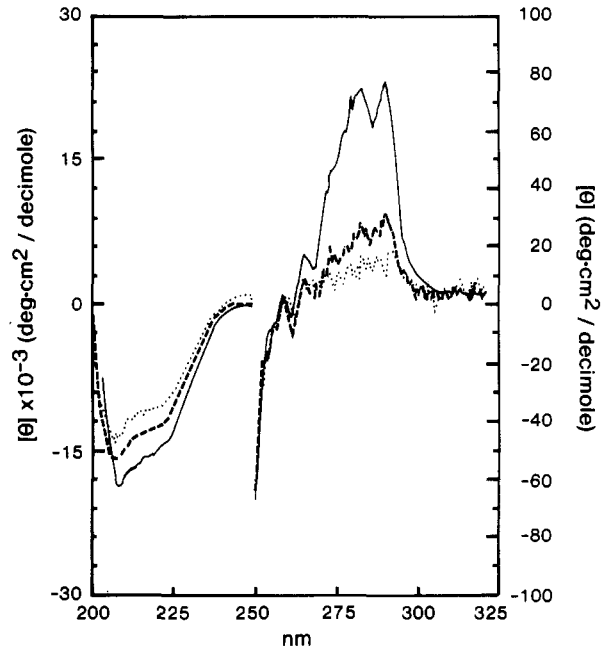

FIGURE 1: Circular dichroic spectra of recombinant EPO at different pHs. Solid line, pH 6.8; dashed line, pH 3.8; dotted line, pH 2.3. The right-hand axis is for the near-UV spectra, and the left-hand axis is for the far-UV spectra.

Density measurements were carried out according to a previously described procedure (Lee et al., 1979) using the Anton Parr DMA-02C precision density meter. The partial specific volume, $\bar{v}$, was calculated by (Cassasa & Eisenberg, 1964)

$$\bar{v} = \frac{1}{\rho_0}\left(1 - \frac{\rho - \rho_0}{c}\right)$$

where ρ_0 is the density of the solvent in grams per milliliter, ρ is the density of the protein solution, and c is the concentration of protein in grams per milliliter. The EPO solutions approximately at 1–3 mg/mL were dialyzed against the buffer, and their densities were determined at 20 °C, maintained by a water bath placed in a constant-temperature room at 20 °C. After the density measurements, the protein solutions were taken from the density meter cell by syringes and protein concentrations determined spectrophotometrically after proper gravimetric dilution with the solvent of known density.

Isoelectric focusing gels contained 5 M urea and 2.5% LKB Ampholines, pH range 3.5–10. A Broadly–James surface electrode was used to measure pHs across the gel.

RESULTS

Structure of Recombinant EPO. The CD spectrum of recombinant EPO is shown in Figure 1. The far-UV spectrum is characterized by a negative minimum at 208 nm and a shoulder around 217 nm. The α-helix content is calculated to be about 50% according to Greenfield and Fasman (1969). The CD spectrum in the near-UV region shows peaks at 290 and 282.6 nm which can be assigned to the tryptophan ^1L_b transition (Strickland, 1974). This suggests that at least one of the three tryptophans is in a fairly rigid environment. Tyrosine probably contributes to the broad signal from about 270 to 280 nm. It is not clear whether phenylalanine is producing positive peaks at 259 and 264 nm or negative peaks at 261.3 and 267.8 nm.

Fluorescence and phosphorescence spectra are shown in Figure 2. The fluorescence emission maximum at 345 nm

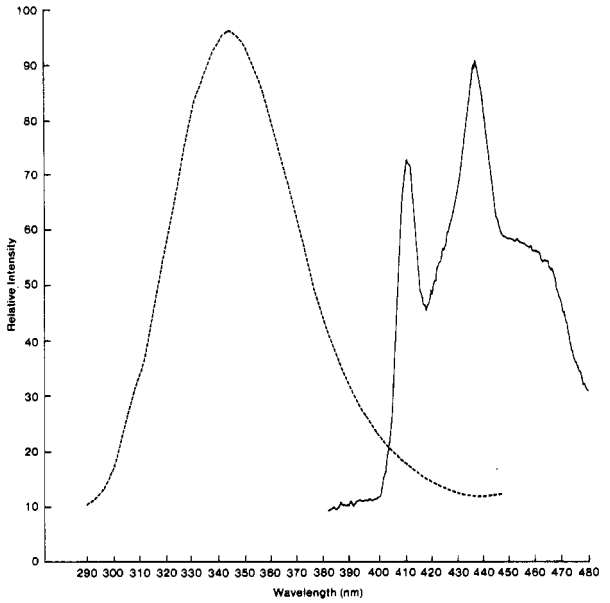

FIGURE 2: Fluorescence and phosphorescence spectra of recombinant EPO. (---) Fluorescence; (—) phosphorescence. Excitation wavelength is 280 nm.

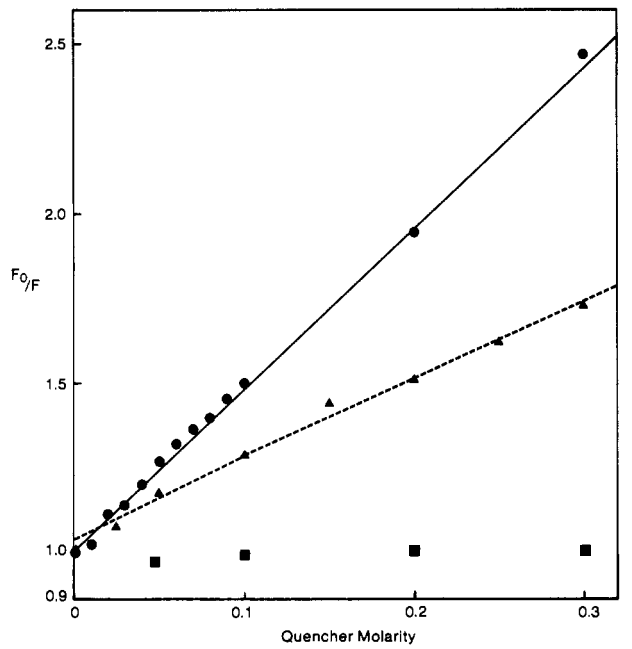

FIGURE 3: Fluorescence quenching of EPO by acrylamide (●), iodide (▲), and cesium (■).

and the full width half-maximum (FWHM) of 55 nm are characteristic of a solvent-exposed tryptophan, as is the phosphorescence zero–zero band at 410 nm (FWHM = 10 nm). Varying the excitation wavelength to 300 nm changed neither the fluorescence nor the phosphorescence spectrum. If such a change had occurred, it would have been evidence for heterogeneity.

Figure 3 shows a direct Stern–Volmer plot of fluorescence quenching by acrylamide, iodide, and cesium. The acrylamide quenching data fit well to a straight line. The slope, which corresponds to the effective quenching constant, K_e, is 4.83 M^{-1}. The y intercept of 1.011 indicates that the fractional assessable fluorescence, f_e, is 99%. The iodide quenching data were also fit to a straight line, since the apparent slight curvature in the plot is of the same magnitude as the scatter in the data. This fit gives $K_e = 2.38\ M^{-1}$ and $f_e = 96.5\%$. Essentially, no quenching by cesium was observed (Figure 3).

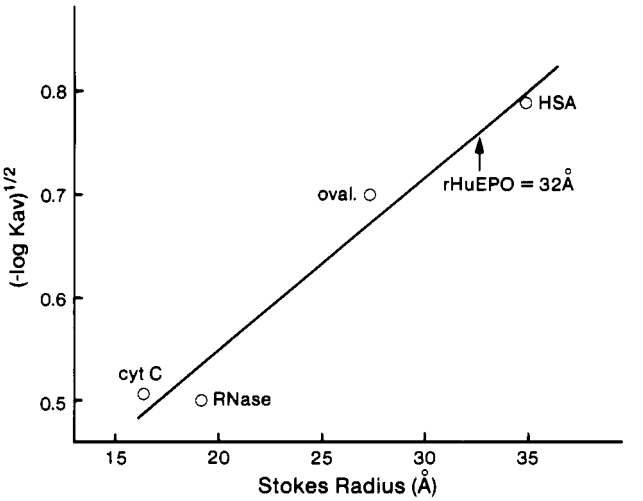

FIGURE 4: Determination of the Stokes radius of recombinant human erythropoietin. Abbreviations: cyt C, cytochrome *c*; RNase, ribonuclease; oval, ovalbumin; HSA, human serum albumin.

Neither the luminescence spectra nor the fluorescence quenching data give any clear evidence for heterogeneity among the fluorophores. This suggests either that all three tryptophans per EPO monomer are in very similar environments or that one tryptophan very strongly dominates the luminescence. All luminescent tryptophans appear to have a high degree of solvent exposure.

It may be of interest to examine the secondary structure of the sequences containing Trp residues. The sequence from Phe-48 to Leu-70, which contains Trp-51 and Trp-64, was examined for amphiphilic orientation of amino acid residues according to Schiffer and Edmundson (1967). This showed a relatively clear orientation of polar and nonpolar residues along the α-helix for this sequence. This, along with a high overall helical potential of the sequence, suggests that this sequence may form an α-helix, one side including Trp-51 facing the solvent. If this is correct, then Trp-51 may be solvent-exposed and Trp-64 buried. The sequence from Trp-88 to Leu-102 showed a relatively high α-helical potential and an amphiphilic orientation with Trp-88 in the hydrophobic side, suggesting that it may also be buried. Comparison of this prediction with the luminescence data suggests that Trp-51 dominates the luminescence and other tryptophans are quenched.

Acid denaturation of EPO was examined by using CD spectra as shown in Figure 1. The UV spectra show a gradual reduction of CD intensity as the pH is lowered. At pH 2.3, the CD intensity is nearly zero, suggesting that the tertiary structure is lost. A plot of the ellipticity at 290 nm against pH shows an apparently cooperative structure transition with the midpoint at pH 4.1. The far-UV spectrum in Figure 4 shows a decrease in the CD intensity. It is evident from the spectrum that considerable secondary structure remains at pH 2.3. Calculation according to Greenfield and Fasman (1969) indicates an α-helix content of approximately 36%, corresponding to about a 30% drop in the α-helix content relative to the native state.

The recombinant CHO derived EPO shows a number of closely spaced bands on an isoelectric focusing gel, with apparent p*I*'s in the range of 4.2–4.6 (data not shown). Nonglycosylated (*Escherichia coli* derived) EPO shows an apparent p*I* of about 9.2. These values are probably slightly higher than the actual p*I*'s because of the presence of urea in the isoelectric focusing gels.

Molecular Weight of EPO. Figure 4 shows the determi-

Table I: Apparent z-Average Molecular Weights Observed as a Function of Centrifugation Speed and Loading Concentration

observation channel	loading concn (g/L)	mol wt ($\times 10^{-3}$) at speed (rpm) 22 000	30 000	40 000
A	0.09	27.1 ± 1.5	30.5 ± 0.7	31.7 ± 0.9
B	0.23	29.8 ± 0.7	30.0 ± 0.2	27.8 ± 0.6
C	0.62	29.5 ± 0.7	30.2 ± 0.2	32.9 ± 1.4

nation of the Stokes radius of recombinant EPO by gel filtration. A graph of the elution parameter, $(-\log K_{av})^{1/2}$, vs. the Stokes radius for the standard proteins shows a reasonable linearity, from which the linear regression line shown was obtained. The value of K_{av} for EPO was determined by gel filtration to be 0.266; this corresponds to a Stokes radius of 32 Å, in reasonable agreement with the value of 33 Å determined for human urinary erythropoietin by O'Sullivan et al. (1970) using the same method.

The partial specific volume of EPO was determined by density measurements in 20 mM sodium citrate, pH 7.0, and 0.1 M NaCl at 20 °C. Four independent measurements gave a value of 0.698 ± 0.004 mL/g with no concentration dependence within experimental error. Such concentration dependence has been observed for the isopotential partial specific volume of many proteins (Arakawa & Timasheff, 1984). This value is significantly lower than the partial specific volume of 0.720 mL/g calculated for the protein moiety only according to Cohn and Edsall (1943), reflecting the glycosylation of recombinant CHO derived EPO. The density of the above solvent, which is also used in the equilibrium experiments, was determined to be 1.006496 g/mL at 20 °C.

Estimates of the apparent z-average molecular weights at three speeds and at three loading concentrations are presented in Table I. In all cases, the fitting deviations from the model (single ideal component) were not systematic, were about 0.025 fringe root mean square, and appeared to reflect random experimental error.

There appears to be no significant dependence of the apparent molecular weight on either speed or loading concentration. Virtually all of the solute present could be observed at 22 000 rpm in channels A and B (with the lower loading concentrations), and nearly all of the solute could be seen in the same channels at 30 000 rpm and in channel A at 40 000 rpm. Thus, the observed molecular weight values in those channels reflect the properties of all of the sample. Since the several values presented in Table I correspond to various concentration ranges, from 2.3 to 15.5 fringes, the relative constancy of the apparent z-average molecular weights indicates that there is no *substantial* nonideality under our experimental conditions.

More precise estimates of molecular weight and nonideality can be obtained by combining data from several channels. Joint fitting of the fringe displacements from all channels at 30 000 and 40 000 rpm to the model of a single ideal component gave a molecular weight of 30 000 ± 300 with fitting deviations of 0.041 fringe root mean square. Similarly, two replicate sets of measurements of all six channels at 22 000 and 30 000 rpm using about 100 data points per channel returned values of 29 810 ± 210 and 29 720 ± 220 for the molecular weight of recombinant EPO with fitting deviations of 0.027 and 0.020 fringes.

More complex fitting models were also tried; in these fits, the data sets were truncated to about 50 points per channel, for convenience. Models assuming monomer–n-mer equilibria (with $n = 2$, 3, or 4) did not improve the fits. However, small decreases in the root mean square of the residuals (less than 0.002 fringe) were obtained by assuming the model of a nonideal single-component system. The returned values of molecular weight and of the second viral coefficient are compared in Table II. The observed nonideality is marginal, consistent with the miniscule reduction in the root mean square of the residuals. The data at 40 000 rpm are particularly susceptible to errors from Wiener skewing (Yphantis, 1964) because of the combination of the long (30 mm) optical path in the centerpiece used here and the steep refractive index gradients at 40 000 rpm. Accordingly, our best estimate of nonideality is from the data at lower speeds: $B = (6.7 \pm 4.8) \times 10^{-4}$ mL mol g^{-2} where the error estimate of the average value is taken as the root mean square average of the individual error ranges. A value of 0.9×10^{-4} mL mol g^{-2} is estimated for the excluded volume contribution to the second viral coefficient of a compact unsolvated spherical molecule of molecular weight 30 000 by using the relation given by Tanford (1961) and our measured value of the partial specific volume. If (as a reasonable upper limit) the glycoprotein is assumed to be a sphere with an exclusion radius twice that of the compact unsolvated sphere, then the predicted value of B rises to 7.2×10^{-4} mL mol g^{-2}. The total estimated (titration) charge on EPO is about 12– at pH 7. Taking the effective charge on this glycoprotein to be 0.45 ± 0.15 times the titration charge [see Johnson and Yphantis (1979) for a discussion], we estimate a contribution of about 0.6×10^{-4} mL mol g^{-2} to the second viral coefficient from Donnan nonideality. Thus, the experimentally observed second viral coefficient of $(6.7 \pm 4.8) \times 10^{-4}$ mL mol g^{-2} appears to be reasonable. More accurate estimation of the value of B would require higher loading concentrations than those (0.009%, 0.02%, and 0.06%) used here.

Table II: Comparisons of Estimated Molecular Weights and Viral Coefficients

data sets for fits	ideal fit (B held at 0), estimated mol wt ($\times 10^{-3}$)	nonideal fit: estimated mol wt ($\times 10^{-3}$)	nonideal fit: second viral coeff, $B \times 10^4$ (mL mol g^{-2})
22K and 30K rpm, set 1	30.0 ± 0.2	30.8 ± 0.5	6.8 ± 3.9
22K and 30K rpm, set 2	29.8 ± 0.2	30.4 ± 0.6	6.6 ± 5.5
30K and 40K rpm	30.0 ± 0.3	29.9 ± 0.4	−0.3 ± 7.9

The possibility of the presence of more than one component was addressed by making use of the combination of the sensitivity of least-squares fitting procedures, the precision of the interference optical system, and the fractionation in the centrifugal field to detect the presence of larger and smaller species (D. A. Yphantis, unpublished results): concentration distributions were visible throughout all of channels A and B at 22 000 rpm, making these data useful for estimations of amounts of any species larger than the principal component. Least-squares fitting of each of these channels to the model of two ideal components showed no evidence of any species with molecular weight above 60 000 (data not shown). Any component present at a weight fraction of 0.005 or more should have been detectable under the conditions of this experiment. Measurements from channel C at 40 000 rpm (where centrifugal disproportion is quite large, leading to considerable enrichment of any smaller species in the region of the cell where interference measurements are possible) make possible estimates of amounts of species smaller than the main component. Under these conditions, a single component of molecular weight from 7000 to 15 000 present at a weight fraction of 0.01 or more should have been detectable. Again, there was no evidence (data not shown) for any component other

than the principal component in the least-squares fitting.

Discussion

It has been reported that the near-UV CD spectrum of urinary EPO has two strong positive bands at 282 and 290 nm and two weak negative bands at 260.5 and 267 nm (Lai et al., 1986). These band positions are essentially identical, within experimental error, with those observed for recombinant EPO in this paper. Since the near-UV CD spectrum is sensitive to alterations in the tertiary structure, the results suggest that the overall conformation is similar for recombinant and urinary EPO preparations. This was further supported by the second derivative of UV absorbance and the fluorescence spectrum. The second-derivative spectrum of recombinant EPO showed two negative peaks at 284 and 292 nm and a positive peak at 288 nm (data not shown), which are identical with those observed for the urinary EPO (T. Arakawa, unpublished results). The fluorescence spectrum of urinary EPO showed an emission peak at 345 nm and FWHM = 56–57 nm (T. Arakawa, unpublished results). These characteristics are identical, within experimental error, with those for recombinant EPO, suggesting a similar environment for at least one of the tryptophan residues in both EPO preparations. In the far-UV CD spectrum, a minimum at 207.5 nm and a shoulder around 218 nm have been reported for urinary EPO (Lai et al., 1986). These characteristics are also similar to those for recombinant EPO in this work, indicating their similar secondary structure. The similarity in the protein conformation is reflected in the similar biological activity (Lin et al., 1985).

Our best estimate of the molecular weight of the recombinant EPO is 30 400 ± 400, interpreting the observed nonideality at 22 000 and 30 000 rpm as being significant. (A slightly lower value, 29 830 ± 170, is obtained by assuming ideal solution behavior.) Since the sequence molecular weight of the protein moiety is 18 399, the weight fraction of carbohydrate for this glycoprotein is estimated to be 0.395 ± 0.008.

The apparent molecular weight of human urinary EPO has been the subject of several reports. Determinations based on gel filtration under nondenaturing conditions or gel electrophoresis in the presence of SDS are not reliable: the former method determines the Stokes radius and not the molecular weight of a protein, and the latter method is, inter alia, confounded by the anomalous behavior of glycoproteins in SDS–polyacrylamide gel electrophoresis (Westphal et al., 1975). At least three different methods with sound theoretical foundations have been used to measure the molecular weight of human urinary EPO in crude mixtures. Radiation inactivation analysis (Rosse et al., 1963), gel filtration in 6 M guanidine hydrochloride (Shelton et al., 1975), and analysis by combined gel filtration and sucrose density ultracentrifugation (O'Sullivan et al., 1970) gave molecular weight values of 27 000, 33 000 ± 2900, and 32 600, respectively. It should be mentioned, however, that the first method was recently shown to give the molecular weight of the protein moiety for the glycoproteins examined, inconsistent with the above value (Kempner et al., 1986). Given the diversity of the test methods, and the assumptions involved in these methods, the previous molecular weight determinations of human urinary EPO are in good agreement with the value of 30 000 determined for recombinant EPO by sedimentation equilibrium.

Equilibrium centrifugation sets upper limits of 0.005 for the weight fraction of any component with a molecular weight twice or more the molecular weight of the main component and of 0.01 for the weight fraction of any component half to one-fourth the size of the principal species, assuming similar buoyancy factors for all species. However, we cannot set useful limits for the amounts of species nearly the same size as the principal species. Thus, we cannot exclude (possibly extensive) heterogeneity of the carbohydrate moiety.

From the molecular weight of recombinant EPO and its partial specific volume, the radius of the EPO molecule was calculated to be 20.2 Å by using a spherical approximation. Comparison of this with the experimental Stokes radius of 32 Å, obtained from gel filtration, suggests two possibilities: EPO either is highly asymmetric or has an expanded structure. Both factors can cause a larger hydrodynamic effective volume and, hence, a larger Stokes radius than for a compact globular protein of the same molecular weight. An expanded structure could result from the three asparagine-linked oligosaccharides found in recombinant EPO. Taking a spherical approximation for the protein moiety of EPO, the radius was calculated to be 17.5 Å. The 14.5-Å difference between the experimental and calculated Stokes radius may be ascribed to the carbohydrate moiety. We speculate that each chain carrying several sugar residues in one direction extends into the solvent and hence significantly increases the Stokes radius. It is known that a free disaccharide molecule has a hydrodynamic effective radius of 4–6 Å (Schachman & Lauffer, 1949; Laurent & Killander, 1964; Arakawa & Timasheff, 1982).

The fluorescence quenching experiments indicate that the tryptophan fluorescence can be quenched by an uncharged (acrylamide) or a negatively charged (iodide) quencher but not by a positively charged one (cesium). Since the protein is negatively charged at pH 7.0 due to sialic acids (p*I* = ~4.4), this observation appears opposite to what is expected. However, this observation may be explained if the net positive charge on the protein moiety (p*I* of nonglycosylated EPO = 9.2), rather than the net negative charge on the whole molecule, is more effective in interacting with ions. It is assumed here that the titration of protein charges is not strongly affected by the sialic acids. This argument may be supported by the observation that the protein is denatured, not stabilized, by lowering the pH below around 4.6. If the overall net charge plays a role in destabilizing the conformation of the molecule, the protein should be more stable at acidic pH (Tanford, 1961). However, we cannot exclude the possibility that positively charged residues are present near the solvent-exposed tryptophan and interfere with quenching by cesium ions.

Acknowledgments

We thank Dr. S. N. Timasheff for use of his density meter, K. Aoki for technical assistance, and J. Bennett for typing the manuscript.

Registry No. Erythropoietin, 11096-26-7.

References

Ansevin, A. T., Roark, D. E., & Yphantis, D. A. (1970) *Anal. Biochem. 34*, 237–261.

Arakawa, T., & Timasheff, S. N. (1982) *Biochemistry 21*, 6536–6544.

Arakawa, T., & Timasheff, S. N. (1984) *Biochemistry 23*, 5912–5923.

Cassasa, E. F., & Eisenberg, H. (1964) *Adv. Protein Chem. 19*, 287–395.

Chang, C.-T., Wu, C.-S., & Yang, J.-T. (1978) *Anal. Biochem. 91*, 13–31.

Cohn, E. J., & Edsall, J. T. (1943) in *Proteins, Amino Acids and Peptides* (Cohn, E. J., & Edsall, J. T., Eds.) p 371, Van Nostrand-Reinhold, Princeton, NJ.

Correia, J. J. (1980) *Fed. Proc., Fed. Am. Soc. Exp. Biol. 39*, 1604.

Correia, J. J. (1983) Ph.D. Thesis, University of Connecticut.

Greenfield, N., & Fasman, G. D. (1969) *Biochemistry 8*, 4108-4116.
Jacobs, K., Shoemaker, C., Rudersdorf, R., Neill, S. D., Kaufman, R., Mufson, A., Seehra, J., Jones, S. S., Hewick, R., Fritsch, E. F., Kawakita, M., Shimizu, T., & Miyake, T. (1985) *Nature (London) 313*, 806-810.
Johnson, M. L., & Yphantis, D. A. (1978) *Biochemistry 17*, 1448-1455.
Johnson, M. L., Correia, J. J., Halvorson, H. R., & Yphantis, D. A. (1981) *Biophys. J. 36*, 575-588.
Kempner, E. S., Miller, J. H., & McCreery, M. J. (1986) *Anal. Biochem. 156*, 140-146.
Kupke, D. W., & Dorrier, T. E. (1978) *Methods Enzymol. 48*, 155-162.
Lai, P.-H., Everett, R., Wang, F.-F., Arakawa, T., & Goldwasser, E. (1986) *J. Biol. Chem. 261*, 3116-3121.
Laue, T. M. (1981) Ph.D. Thesis, University of Connecticut.
Laue, T. M., & Yphantis, D. A. (1979) *Biophys. J. 25*, 164a.
Laue, T. M., Yphantis, D. A., & Rhodes, D. G. (1984) *Anal. Biochem. 143*, 102-112.
Laurent, T. C., & Killander, J. (1964) *J. Chromatogr. 14*, 317-330.
Lee, J. C., Gekko, K., & Timasheff, S. N. (1979) *Methods Enzymol. 61*, 26-49.
Lehrer, S. S., & Leavis, P. C. (1978) *Methods Enzymol. 49*, 222-236.
Lin, F.-K., Suggs, S., Lin, C.-H., Browne, J., Smalling, R., Egrie, J., Chen, K., Fox, M., Stabinsky, Z., Badrawi, S., Lai, P.-H., & Goldwasser, E. (1983) *Proc. Natl. Acad. Sci. U.S.A. 82*, 7580-7584.
Miyake, T., Kung, C. K.-H., & Goldwasser, E. (1977) *J. Biol. Chem. 252*, 5558-5564.
Ogston, A. G. (1958) *Trans. Faraday Soc. 54*, 1754-1757.
Olesen, H., & Foch, J. (1968) *Scand. J. Haematol. 5*, 211-214.
O'Sullivan, M. B., Chiba, Y., Gleich, G. J., & Linman, J. W. (1970) *J. Lab. Clin. Med. 75*, 771-779.
Paul, C. H., & Yphantis, D. A. (1972) *Anal. Biochem. 48*, 588-604.
Rosse, W. F., Berry, R. J., & Waldmann, T. A. (1963) *J. Clin. Invest. 47*, 124-129.
Schachman, H. K., & Lauffer, M. A. (1949) *J. Am. Chem. Soc. 71*, 536-541.
Schiffer, M., & Edmundson, A. B. (1967) *Biophys. J. 7*, 121-135.
Shelton, R. N., Ichiki, A. T., & Lange, R. D. (1975) *Biochem. Med. 12*, 45-54.
Strickland, E. H. (1974) *CRC Crit. Rev. Biochem. 47*, 251-276.
Tanford, C. (1961) *Physical Chemistry of Macromolecules*, pp 195-229, Wiley, New York.
van Holde, K. E., & Baldwin, R. L. (1958) *J. Phys. Chem. 62*, 734-743.
Westphal, U., Burton, R. M., & Harding, G. B. (1975) *Methods Enzymol. 36*, 91-104.
Yphantis, D. A. (1964) *Biochemistry 3*, 297-317.
Yphantis, D. A., Laue, T. M., & Anderson, I. (1984) *Anal. Biochem. 143*, 95-102.

Stereoselective Covalent Binding of Enantiomers of *anti*-Benzo[*a*]pyrene Diol Epoxide to DNA As Probed by Optical Detection of Magnetic Resonance†

Vassily Kolubayev,‡ Henry C. Brenner,* and Nicholas E. Geacintov
Department of Chemistry, New York University, New York, New York 10003
Received October 30, 1986; Revised Manuscript Received January 5, 1987

ABSTRACT: Phosphorescence and optical detection of magnetic resonance measurements applied to the covalent adducts of (+)- and (−)-*anti*-benzo[*a*]pyrene with DNA show a marked red shift of the pyrenyl phosphorescence and a lowering of the zero field splitting parameters of the (−) adduct, relative to the (+) adduct and the (solvent-exposed) benzo[*a*]pyrene tetraol. These results are consistent with a predominance of quasi-intercalative sites in the (−) adduct and external, solvent-exposed sites in the (+) adduct.

The two enantiomers of *trans*-7,8-dihydroxy-*anti*-9,10-epoxy-7,8,9,10-tetrahydrobenzo[*a*]pyrene (BaPDE,[1] Figure 1) are characterized by remarkably different tumorigenic and mutagenic activities (Conney, 1982; Harvey, 1981). The biological effects of these (and other) reactive polycyclic aromatic hydrocarbon metabolites are believed to involve the formation of adducts derived from the covalent binding of BaPDE to DNA (Singer & Grunberger, 1983; Brookes & Osborne, 1982). It is therefore of great interest to determine if there are any significant differences in the conformations and properties of the adducts derived from the binding of the (+) and (−) enantiomers of BaPDE to double-stranded DNA, which might ultimately provide an insight into the biochemical activities of these compounds on a molecular level.

In the last few years, optical detection of magnetic resonance (ODMR) has been employed as a probe of the structure of complexes of DNA with polycyclic aromatic hydrocarbon carcinogens (Chiha et al., 1977, 1978; Lefkowitz et al., 1979; Lefkowitz & Brenner, 1981, 1982; Clarke et al., 1983). As is well-known, the excited triplet state of an organic molecule

† Research supported by Grant CA 20851, awarded by the National Cancer Institute, DHHS, to N.E.G. and H.C.B. and by Grant DE-FG02-86ER60405 from the Department of Energy.
* Author to whom correspondence should be addressed.
‡ Present address: Molecular Dynamics Section, Chemistry Division, U.S. Naval Research Laboratory, Washington, DC 20375.

[1] Abbreviations: BaPDE, *trans*-7,8-dihydroxy-*anti*-9,10-epoxy-7,8,9,10-tetrahydrobenzo[*a*]pyrene; BaPT, 7,8,9,10-tetrahydroxytetrahydrobenzo[*a*]pyrene; BeP, benzo[*e*]pyrene; BePE, 9,10-epoxy-9,10,11,12-tetrahydrobenzo[*e*]pyrene; DNA, deoxyribonucleic acid; EGB, ethylene glycol/buffer solution; GHz, gigahertz; MHz, megahertz; ODMR, optically detected magnetic resonance.

0006-2960/87/0426-2638$01.50/0